Ceramics International 44 (2018) 4868–4874

Contents lists available at ScienceDirect

Ceramics International

journal homepage: www.elsevier.com/locate/ceramint

Sintering, microstructure and hardness of Y-TZP- 64S bioglass ceramics

Clara G. Soubelet, María P. Albano*, María S. Conconi

Centro de Tecnología de Recursos Minerales y Cerámica (CETMIC), C.C. 49 (B1897ZCA) M. B. Gonnet, Provincia de Buenos Aires, Argentina

ARTICLE INFO

Keywords:
Y-TZP- (64S) bioglass compacts
Sintering
Phase evolution
Microstructure
Hardness

ABSTRACT

3 mol% yttria-partially stabilized zirconia (Y-TZP) powder and a sol-gel derived CaO- P_2O_5- SiO_2 (64S) bioglass, were used to produce Y-TZP- 64S slip cast compacts. The compacts with 10.5 and 19.9 vol% 64S were sintered at different temperatures up to 1500 °C using 5 and 10 °C/min heating/cooling rates. The densification behaviour, crystalline phase formation and zirconia grain growth were investigated as a function of sintering temperature and 64S glass content. $Ca_3(PO_4)_2$ along with SiO_2 as a major phase were obtained from thermal decomposition of the 64S glass at 950–1500 °C. Both 64S additions, 10.5 and 19.9 vol%, promoted the sintering process at a lower temperature with respect to Y-TZP (1500 °C); the SiO_2 phase markedly increased the Y-TZP solid state sintering rate at the intermediate stage. The rapidly cooling at 10 °C/min inhibited the t-m transformation of Y-TZP and markedly reduced that of Y-TZP- 64S at 1300–1500 °C. Sintered Y-TZP with 10.5 vol% 64S, nearly fully densified at 1300–1400 °C, was constituted by polygonal $ZrSiO_4$ particles and elongated $Ca_2P_2O_7$ particles uniformly distributed in the tetragonal zirconia fine grain matrix. This ceramic exhibited similar hardness to that of Y-TZP sintered at 1500 °C; the in situ formation of calcium phosphate will have the potential to improve the Y-TZP biological properties without significantly affecting its hardness.

1. Introduction

3 mol% yttria-partially stabilized zirconia (Y-TZP) ceramics produced using bioglass additives, are currently of great interest for dental applications, as an alternative to metal and resin prosthesis or parts in restorations. Y-TZP bioceramics have a combination of favourable properties such as high strength, abrasion resistance, good biocompatibility and aesthetics [1].

Dense Y-TZP ceramics are usually fabricated by solid state sintering at high temperatures of around 1500–1600 °C. It has been reported by several researchers [2,3] that Y-TZP densification is enhanced by the addition of frit glasses which form a viscous flow during the sintering process. Most of the glass compositions used contain significant amounts of alkali oxides [4]; the disadvantage of these glass compositions in colloidal forming techniques such as slip casting, is the high dissolution rate of the glass in aqueous media that make them unsuitable for preparing stable concentrated aqueous Y-TZP-glass suspensions. The present investigation used an alkali-free bioglass in the CaO- P_2O_5- SiO_2 system, formed by the sol-gel technique, with a composition: 64 mol% SiO_2, 26 mol% CaO, 10 mol% P_2O_5 (64S), as an additive for Y-TZP. Our experiments have proved that this composition is refractory, i.e. it did not melt at the sintering temperatures (1300–1500 °C), therefore the in-situ formation of a Ca containing crystalline phase in the Y-TZP matrix will be expected. The aim of this work was to develop a ceramic constituted by zirconia grains and small amounts of a Ca containing secondary phase, that may improve the Y-TZP biological properties without significantly affecting its mechanical properties.

Y-TZP- 64S slip cast compacts with 10.5 and 19.9 vol% 64S were sintered at different temperatures up to 1500 °C using 5 and 10 °C/min heating/cooling rates. It is generally accepted [5] that the tetragonal (t) to monoclinic (m) zirconia transformation is strongly dependent on its grain size, this transformation would be inhibited in a fine zirconia grain microstructure. The type of glass used in terms of composition and synthesis method is expected to affect the sintering behaviour as well as the microstructure of Y-TZP ceramics. In this work, the phase evolution of the 64S glass during thermal treatment was analysed by Rietveld method, in order to determine the influence of the different phases on the sintering and microstructure of Y-TZP- 64S ceramics. The densification behaviour, crystalline phase formation and Y-TZP grain growth were investigated as a function of sintering temperature and 64S glass content. In addition, the effect of the heating/cooling rate on the Y-TZP grain coarsening and stability of the tetragonal phase was evaluated. Finally, the hardness of sintered Y-TZP and Y-TZP- 64S samples were compared.

* Corresponding author.
E-mail address: palbano@cetmic.unlp.edu.ar (M.P. Albano).

https://doi.org/10.1016/j.ceramint.2017.12.076
Received 8 September 2017; Received in revised form 29 November 2017; Accepted 11 December 2017
Available online 14 December 2017

2. Experimental procedure

2.1. Raw materials and powder processing

3 mol% yttria- partially stabilized zirconia (Y-TZP) (Saint-Gobain ZirPro, Chine) powder with more frequent particle diameters of 0.14 and 0.48 μm (measured using a Mastersizer 2000, Malvern Instruments, UK), was used in this study. The sol-gel synthesis of the glass in the CaO- P_2O_5- SiO_2 system with composition: 64% SiO_2, 26% CaO and 10% P_2O_5 (mol%) was performed as follows: initially, tetraethoxysilane (TEOS, Aldrich) was added to 0.1 M nitric acid and the mixture was allowed to react for 60 min for the acid hydrolysis of TEOS. Then, a series of reagents were added in the following sequence: triethylphosphate (TEP, Aldrich) and calcium nitrate tetrahydrate (Aldrich), allowing 45 min for each reagent to react completely. After the final addition, mixing was continued for 1 h for the completion of the hydrolysis. The resultant solution was kept in a sealed container for 10 days at room temperature to allow gelation to occur and subsequently heated at 70 °C for an additional 3 days. Afterwards, the water was removed and a small hole was inserted in the lid to allow the leakage of gases while the gel was heated at 120 °C for 2 days. The dried gel was then heated at 700 °C for 24 h to stabilize the glass and eliminate residual nitrates. The stabilized glass powder was milled in an attrition mill using 1.6 mm zirconia balls during 48 h. This bioglass powder, subsequently referred as 64S, with a mean particle diameter of 3.0 μm (determined using a Mastersizer 2000) was used for the experiments presented in this study; its measured density was 2.70 g/cm^3.

Three different zirconia ceramics were investigated in this study. The three materials were pure 3 mol% yttria- partially stabilized zirconia (Y-TZP), Y-TZP with 10.5 vol% 64S (Y-TZPA) and Y-TZP with 19.9 vol% 64S (Y-TZPB). A commercial ammonium polyacrylate solution (Duramax D 3500, Rohm & Haas, Philadelphia PA) was used as deflocculant. 43 vol% aqueous Y-TZP and Y-TZP-64S suspensions with the different compositions and the optimum NH_4PA concentration were prepared by suspending particles in deionized water via 40 min of ultrasound; when it was necessary the pH was manually adjusted to be maintained at 9 with ammonia (25%). Slips were cast in plaster molds into disks of diameter 1.85 cm. The consolidated disks were dried slowly in air for 24 h at room temperature and 24 h at 100 °C. The resulting green compacts were sintered in the temperature range of 1100–1500 °C for 2 h in air, with heating/cooling rates of 5 and 10 °C/min.

2.2. Characterization techniques

The infrared spectrum of the glass was obtained using a Fourier transform infrared spectrometer (FTIR) (Equinox 55, USA) using a 4 cm^{-1} resolution over the 400–1400 cm^{-1}region. Differential thermal analysis (DTA) of the stabilized glass powder was performed in air (STA 409, Netzsch Inc., Germany) from room temperature to 1450 °C at a heating rate of 10 °C/min with α-alumina as a reference material.

Crystalline and amorphous phases evolution was characterized by X-ray diffraction (Bruker, D2 Phaser, with Kα: Cu as incident radiation and Ni filter). The equipment was operated at 30 kV and 10 mA and the scanning was performed with a step of 0.04° and 2.5 s per step in the 2θ range between 10° and 80°. The XRD patterns were analysed with PROGRAM FullProf.2k (Version 5.80 - May 2016-ILL JRC) which is a multipurpose profile-fitting program, including Rietveld refinement method, to perform phase quantification [6,7]. Non crystalline phase was quantified applying the Le Bail approach including it in the Rietveld refinement as a crystalline phase adopting a faulted structural model due to very small crystallite size [8]. In this work, the cubic silica with Space Group $P2_13$ was selected to describe de glass.

The bulk density of the sintered compacts was determined with the Archimedes method using distilled water as the immersion liquid. A theoretical density of 6.05 g/cm^3 was used to calculate the relative density of Y-TZP. The theoretical density of the sintered Y-TZP- 64S compacts at each temperature was calculated from the volume fraction of the different phases and their respective density values. The volumetric shrinkage was determined from the dimensions of green and sintered bodies. The sintered samples were polished with a series of diamond paste up to 3 μm. The Vickers hardness (Hv) was carried out using a diamond indenter (Buehler hardness tester) with a load of 3 Kgf and a holding time of 15 s. Hv was calculated as:

$$Hv = 1.854\frac{F}{d^2} \quad (1)$$

F is the indentation load and d is the arithmetic mean of two diagonals (d_1 and d_2). The reported Hv values are the average and standard deviation of ten indentations.

The morphology and composition of the phases were studied using a scanning electron microscopy (SEM) (FEI, Quanta 200) attached with energy dispersive x-ray spectrometer (EDS). Polished specimens were thermally etched for 30 min at a temperature 50 °C below each sintering temperature. SEM images were used to measure the average zirconia (ZrO_2) grain sizes of the sintered compacts using Image J software according to the linear interception method. The reported grain sizes were the average of at least 200 grains.

3. Results and discussion

3.1. Glass characterization and thermal treatment

The XRD pattern of the glass powder (Fig. 1) exhibited a broad amorphous halo indicating the absence of any crystallinity at 700 °C. The infrared spectrum of the 64S glass is shown in Fig. 2. The stretching strong vibrational band of SiO_4 tetrahedron at ~1070 cm^{-1} was the main IR band. Besides, a low frecuency band centered at ~ 470.5 cm^{-1} along with another one at 804 cm^{-1}, ascribed to Si-O-Si bending vibration were presented. A small broad band at ~ 565.7 cm^{-1} was also found which corresponded to P-O bending vibration in a PO_4^{-3} tetrahedron. Two stretching vibrational shoulders of PO_4^{-3} centered at ~ 930 and 1220 cm^{-1} were also detected. Sinkó et al. [9] studied the assessment of the phosphorous precursor´s effect on the bond systems in calcium phosphate silicate (CaPSi) glasses. They demonstrated that CaPSi produced from TEP in acidic medium possess Ca ions connect to phosphorous rather than silicon in an orthophosphate-type environment. Goel et al. [10] explained that alkali-earth cations have higher affinity for phosphate groups, removing the modifiers cations out of the silicate network, thereby inducing polimerization of the silicate glass network.

The DTA plot of the glass powder, shown in Fig. 3, showed two exothermic peaks at 863 °C and 1298 °C attributed to the formation of two different crystalline phases. Fig. 4 presents the quantity of

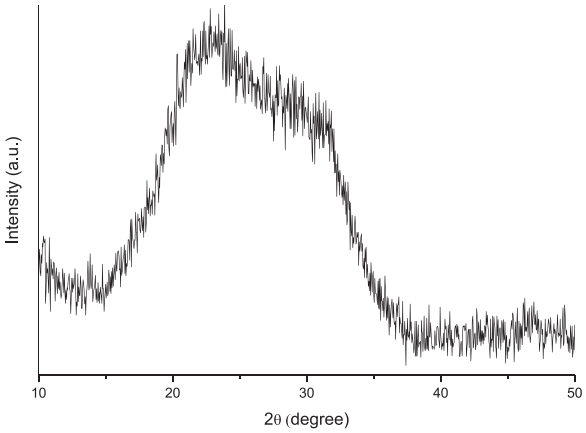

Fig. 1. XRD pattern of 64S glass.

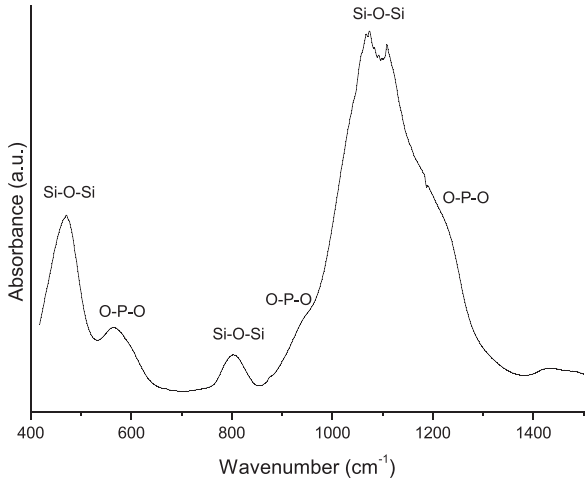

Fig. 2. Infrared spectrum of 64S glass.

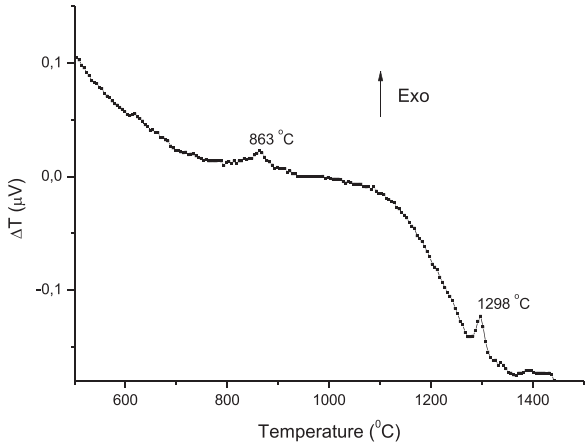

Fig. 3. DTA curve of 64S glass.

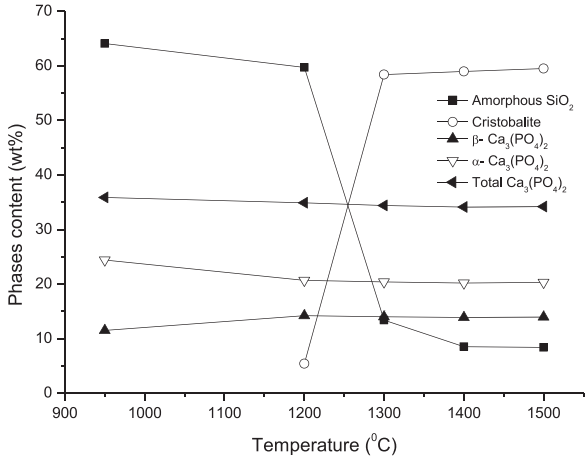

Fig. 4. Amorphous and crystalline phase contents during 64S annealing, as a function of the calcination temperature. The duration time at each temperature is 2 h.

amorphous and crystalline phases during 64S annealing, as a function of the calcination temperature from 950 to 1500 °C; the Rwp parameters obtained in all the cases were satisfactory (below 30) taking in account the presence of low crystallinity and non crystalline phases.

The appearance of α and β- $Ca_3(PO_4)_2$ (TCP) at 950 °C could be detected, thus the exothermic DTA peak at 863 °C (Fig. 3) corresponded to the simultaneous crystallization of α and β –TCP, leaving amorphous SiO_2 as a major phase up to ~1250 °C. This result indicated that Ca

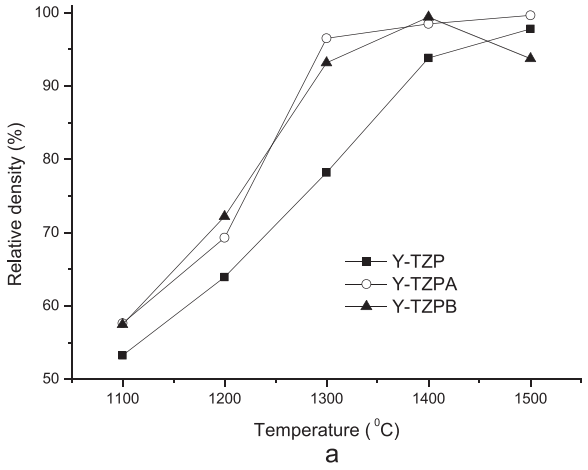

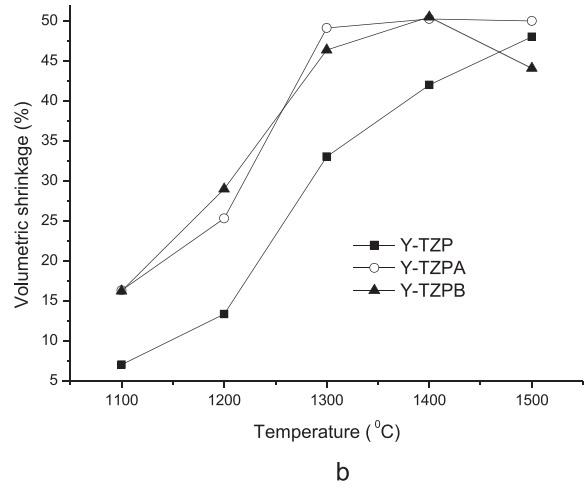

Fig. 5. Relative density (a) and volumetric shrinkage (b) of Y-TZP, Y-TZPA and Y-TZPB, as a function of the sintering temperature at heating rate of 5 °C/min.

tends to associate preferentially with phosphorous which consequently let to the formation of amorphous SiO_2. The exothermic DTA peak at 1298 °C was associated to the crystallization of cristobalite at the expense of amorphous SiO_2. However, amorphous SiO_2 still persisted in the composition as a minor phase along with cristoballite and TCP up to 1500 °C (Fig. 4). Thus, at temperatures ≥ 1300 °C nearly fully crystalline phases consisting of cristoballite, α and β –TCP, and 8–12 wt% of SiO_2 amorphous were measured. The 2.12 α/β ratio at 950 °C decreased up to 1200 °C and then remained nearly constant with further increasing in calcination temperature. The total quantity of TCP (α + β) was almost constant at 950–1500 °C, having a value of ~ 34–35 wt%.

3.2. Densification, microstructure and hardness of Y-TZP and Y-TZP- 64 S

Figs. 5a and 5b show the relative density and the volumetric shrinkage, respectively, of Y-TZP, Y-TZPA and Y-TZPB as a function of the sintering temperature at heating rate of 5 °C/min. The temperature dependence of the relative density and volumetric shrinkage of Y-TZP, Y-TZPA and Y-TZPB at 10 °C/min heating rate, were similar to those obtained at 5 °C/min.

The relative density of Y-TZPA and Y-TZPB and the respective volumetric shrinkage were higher than those of Y-TZP in the temperature range of 1100–1400 °C. This result revealed that the densification of Y-TZP powder was accelerated by the addition of 64S glass. It has been reported [2] that densification of Y-TZP during the sintering process is enhanced by the addition of frits glass which form a viscous flow at

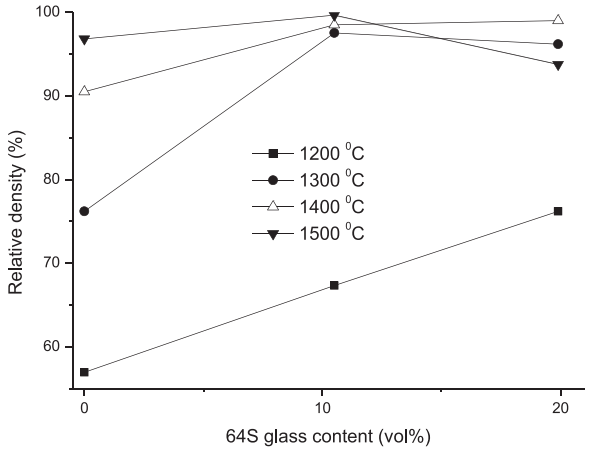

Fig. 6. Relative density of the samples, sintered at 10 °C/min heating rate, as a function of the 64S glass content for different sintering temperatures.

1200–1300 °C. Taking into account that in the present study the sol-gel 64S glass did not form a viscous flow in the temperature range examined, the major SiO_2 phase produced during 64S annealing (Fig. 4) markedly increased the Y-TZP solid state sintering rate. Matsui [11] has investigated the effect of SiO_2 addition on the initial sintering stage of Y-TZP powders; he concluded that SiO_2 changes the diffusion mechanism from grain-boundary to volume diffusion at the initial sintering stage. The increase of sintering rate by SiO_2 addition is attributed to the increase in the apparent frecuency-factor term in the rate constant [11].

In the present study, the relative density of Y-TZP increased with increasing sintering temperature and reached 98% of the theoretical density (T. D.) at 1500 °C. Nearly full densification of Y-TZPA was found at 1300 °C, whereas the highest sintered density for Y-TZPB occurred at 1400 °C. Thus, the maximum densification was clearly dependent on the amount of 64S added; 10.5 vol% 64S promoted the sintering process at a lower temperature.

Fig. 6 shows the relative density of the samples, sintered at 10 °C/min heating rate, as a function of the 64S glass content for the different sintering temperatures; similar relative density vs. 64S content curves were obtained at 5 °C/min heating rate. When the relative density values of the samples were lower than ~96% T. D., the sintering step corresponded to the intermediate stage. This behaviour occurred at temperatures between 1200 and 1300 °C for Y-TZP-64S and 1200–1400 °C for Y-TZP. At the intermediate stage of sintering, the presence of SiO_2 provided a rapid diffusion path between the particles in which mass transfer took place, as a result the Y-TZP densification was enhanced. At 1400 °C, Y-TZP with the two 64S glass contents attained the final sintering stage (relative densities > 96% T. D.), at this stage the sintered density was not dependent on the amount of glass added. The same behaviour occurred at 1500 °C up to 10.5 vol% 64S added, further increase in the amount of glass produced a decrease in the relative density. This behaviour will be explained in subsequently paragraphs.

XRD measurements and Rietveld calculations were performed to investigate the influence of the sintering temperature, in the range of 1300–1500 °C, on the formation of crystalline phases in the different samples (Fig. 7). Fig. 7a shows the monoclinic ZrO_2 (m- ZrO_2) content as a function of the sintering temperature for Y-TZP, Y-TZPA and Y-TZPB at heating/cooling rates of 5 and 10 °C/min. At 5 °C/min, the addition of 64S induced the formation of m-ZrO_2 in the temperature range studied; it was clearly observed that the t-m transformation increased with both the sintering temperature and the glass content. The m-ZrO_2 content of all the samples slightly increased with increasing temperature from 1300 to 1400 °C, a further increase in temperature up to 1500 °C enhanced the t-m transformation. At each temperature, the

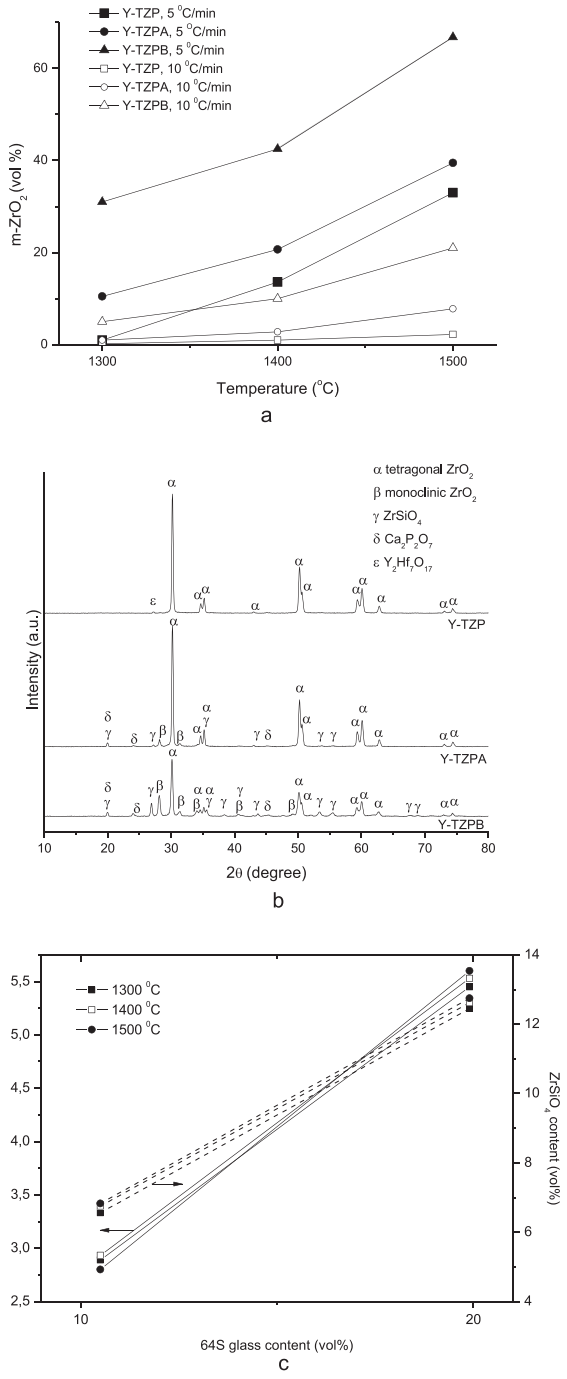

Fig. 7. (a) Monoclinic ZrO_2 content as a function of the sintering temperature for the different samples at heating/cooling rates of 5 and 10 °C/min; (b) XRD patterns of Y-TZP, Y-TZPA and Y-TZPB compacts sintered at 1400 °C (10 °C/min heating/cooling rates); (c) $ZrSiO_4$ and $Ca_2P_2O_7$ contents vs. 64S glass content in Y-TZP-64S compacts sintered at 1300–1500 °C (10 °C/min heating/cooling rates).

increase in the 64 S content from 0 to 10.5 vol% produced a scarcely increased in the m- ZrO_2 content, whereas a more pronounced t-m transformation was found for 19.9 vol% 64S addition. Thus, the difference in the m- ZrO_2 content between Y-TZP and Y-TZP-64S became larger as the 64S content increased from 10.5 to 19.9 vol%.

The increase in the heating/cooling rates from 5 to 10 °C/min inhibited the t-m transformation of Y-TZP and Y-TZPA at 1300–1500 °C and 1300–1400 °C, respectively, and markedly reduced that of Y-TZPB in the range 1300–1500 °C (Fig. 7a); resulting in materials mostly constituted by tetragonal ZrO_2 (t- ZrO_2) grains. At 1500 °C, the m- ZrO_2

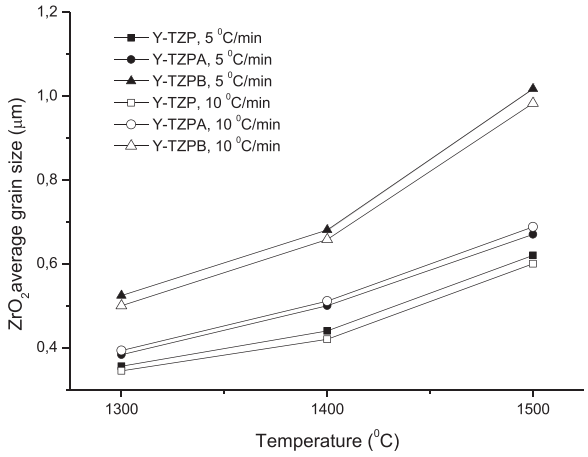

Fig. 8. ZrO_2 average grain size as a function of the sintering temperature for different samples sintered at 5 and 10 °C/min heating rates.

appeared for the compositions with 64S glass, exhibiting a less pronounced t-m transformation for Y-TZPA with respect to Y-TZPB. According to Piconi [5], the fraction of t- phase retained at room temperature in ZrO_2 ceramics is dependent on both the grain size and the yttria content. XRD measurements of Y-TZP at 1400 °C (Fig. 7b) revealed the presence of traces of $Y_2Hf_7O_{17}$, Y^{3+} and Hf^{4+} included in the starting ZrO_2 powder segregated to grain-boundaries; Sakka et al. [12] also reported the cation diffusion to grain boundaries in Y_2 O_3 -$(Z_{r1-x}$ $Hf_x)O_2$ systems. In the present study, a nearly constant yttria content (2.3–2.5 mol%), estimated by using EDS analysis, in the ZrO_2 grains was measured at 1300–1500 °C; as a consequence, the fraction of m-ZrO_2 was considered to be only dependent on the ZrO_2 grain sizes.

The relationship between the ZrO_2 average grain size in the different samples and the sintering temperature, at 5 and 10 °C/min heating rates, is presented in Fig. 8. At 5 °C/min, the ZrO_2 main grain size of Y-TZP gradually increased up to 1400 °C and then rapidly with further increasing in temperature up to 1500 °C. Ohmichi et al. [13] studied the influence of the sintering temperature on the grain size of Y-TZP sintered at 1300–1500 °C, the increasing tendency in the grain size with temperature obtained in the present work agrees well with that reported by Ohmichi et al. The ZrO_2 grain size did not significantly increase by the presence of 10.5 vol% 64S; however, 19.9 vol% 64S addition promoted the ZrO_2 grain growth with a similar temperature dependence to that of Y-TZP, the ZrO_2 grain size increased from 0.68 to 1.02 μm as the temperature increased from 1400 to 1500 °C. Piconi et al. [5] demonstrated that a critical grain size exists above which spontaneous t-m transformation occurred. The tetragonal phase became easier to transform with increasing their size promoting the t-m transformation with increasing the 64 S content from 10.5 to 19.9 vol% at 1300–1500 °C (Figs. 7a and 8).

At 10 °C/min, similar ZrO_2 grain sizes with respect to those obtained at 5 °C/min were measured at 1300–1500 °C for the different sintered compacts (Fig. 8). Since the ZrO_2 grain growth during the heating cycle at both heating rates studied was similar, it could be concluded that the faster cooling cycle (10 °C/min) let to a greater stability of the tetragonal phase reducing the t-m transformation of Y-TZP, Y-TZPA and Y-TZPB at the whole temperature range examined (Fig. 7a).

XRD results (Fig. 7b) showed that during sintering of Y-TZPA and Y-TZPB compacts the formation of $ZrSiO_4$ and $Ca_2P_2O_7$ occurred along with t and m- ZrO_2, TCP traces were also detected (not shown). $ZrSiO_4$ was not found at temperatures lower than 1300 °C. SEM images of Y-TZPA at 1400 and 1500 °C (Figs. 9a and 9c) show sharped edges particles, and elongated ones, distributed in the Y-TZP matrix. The EDS spectrum of the polygonal particles having sharped edges (A) indicated the presence of Si along with Zr and O (Fig. 9e). The molar ratio Si/Zr estimated by EDS analysis was about 1 which corresponded to that of $ZrSiO_4$. The EDS spectrum of the elongated particles (B) (Fig. 9f) had sharp signals for O, P and Ca, low intensity signals of Si, Zr and O belonged to the ZrO_2 matrix and $ZrSiO_4$. The 2.01 keV signal intensity mainly corresponded to P since the Zr contribution to its intensity was very low. The EDS analysis of the B particles revealed that the molar ratio Ca/P was close to 1 corresponding to that of $Ca_2P_2O_7$.

$ZrSiO_4$ and $Ca_2P_2O_7$ contents for 10.5 and 19.9 vol% 64S additions, in Y-TZP-64S compacts sintered at 1300–1500 °C (10 °C/min heating/cooling rates), is presented in Fig. 7c. Similar $ZrSiO_4$ and $Ca_2P_2O_7$ contents vs. 64S glass content curves were obtained at 5 °C/min heating/cooling rates. In addition to these crystalline phases, ~ 1.0 and 2.1 vol% of a SiO_2- based amorphous phase was detected in the compositions with 10.5 and 19.9 vol% 64S, respectively, at 1300–1500 °C. These results were correlated with the phase evolution of the annealed 64S glass (Fig. 4); it was previously demonstrated that SiO_2 was produced as the major phase during 64S thermal treatment, most of the SiO_2 reacted with ZrO_2 leading to the formation of $ZrSiO_4$ and a low amount of amorphous SiO_2 persisted in the compacts sintered at 1300–1500 °C. For each Y-TZP-64S composition, $ZrSiO_4$ and $Ca_2P_2O_7$ contents were almost the same irrespective of the sintering temperature. However, an increase in the $ZrSiO_4$ content from ~ 6.7–12.6 vol% and $Ca_2P_2O_7$ from ~ 2.8–5.6 vol% were measured as the 64S content increased from 10.5 to 19.9 vol%, respectively. This behaviour was in accordance with the greater amounts of SiO_2 and calcium phosphate produced by the glass decomposition for Y-TZPB compacts. Thus, the 64S glass content was the main factor affecting the development of $ZrSiO_4$ and $Ca_2P_2O_7$ phases.

Larger ZrO_2 grain sizes with increasing 64S content from 0 to 19.9 vol% could be found at 1500 °C (10 °C/min heating/cooling rates) (Figs. 8 and 9b-9d). The grain growth mechanism in Y-TZP can be understand from Ostwald ripening that is controlled by lattice diffusion of cations [14]. The Y-TZP grain size became larger at higher sintering temperatures as a consequence of the faster diffusion of Y^{+3} ions. Similar results pertaining the role of Y^{+3} ions on Y-TZP sintered at 1300–1500 °C have been reported by Matsui et al. [15]. Zhao et al. [14] used Y-TZP doped with 5 wt% of colloidal SiO_2 to estimate the effect of SiO_2 grain-boundary phase on the Y-TZP grain growth behaviour. They observed that the amorphous SiO_2 was absent in most grain boundaries and was located only at grain-boundary corners and triple-grain junctions at temperatures < 1600 °C. Therefore, in their work the presence of a SiO_2 phase did not enhance the grain growth of Y-TZP. On the contrary, in the present study, the presence of a SiO_2-based amorphous phase along grain boundary faces in Y-TZP-64S sintered compacts was expected, promoting grain coarsening at the final sintering stage. The greater grain growth (average grain size ~ 1 μm) for Y-TZPB at 1500 °C (Fig. 8) produced a separation between Y-TZP grains resulting in residual porosity (Fig. 9d) and a markedly decreased in the relative density as shown in Figs. 5a and 6.

Fig. 10 shows the Vickers hardness (H_v) as a function of the sintering temperature for Y-TZP, Y-TZPA and Y-TZPB (10 °C/min heating/cooling rates). For Y-TZP, the hardness increased with increasing sintering temperature from 1300 to 1500 °C as a consequence of the increase in the relative sintered density (Fig. 6). For Y-TZPA, the hardness values were similar in the range of temperatures studied in accordance with the sintered density results. In contrast, the H_v vs. temperature curve for Y-TZPB showed a maximum at 1400 °C; when the temperature increased from 1400 °C to 1500 °C a decrease in the relative sintered density attributed to the ZrO_2 grain growth occurred (Figs. 6 and 8). There is a relation between the hardness and the grain size [16], the H_v increased with decreasing the grain size (G) (e. g., $H_v \propto G^{-1}$). As the ZrO_2 average grain size of Y-TZPB at 1500 °C was about 1 μm a markedly decreased in the H_v values was found.

The H_v values of Y-TZP at 1400–1500 °C were not significantly reduced by the addition of 10.5 vol% 64S (Fig. 10); thus, Y-TZPA nearly fully densified at 1300–1500 °C (Fig. 6) exhibited similar H_v values to that of Y-TZP at 1500 °C. However, Y-TZPB having the highest sintered

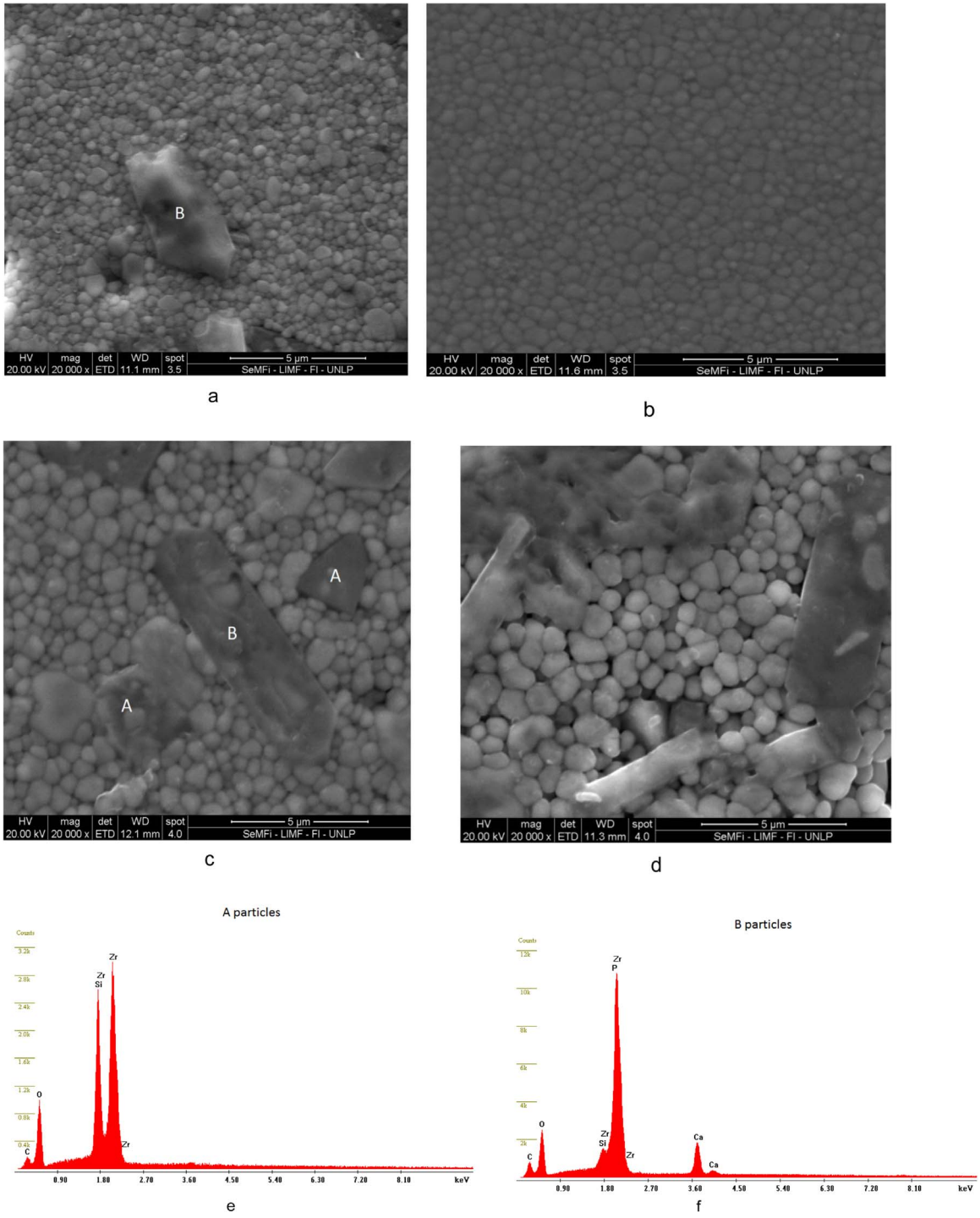

Fig. 9. (a-d) SEM micrographs of different sintered compacts: Y-TZPA at 1400 °C (a), Y-TZP at 1500 °C (b), Y-TZPA at 1500 °C (c), Y-TZPB at 1500 °C (d); (e, f) EDS spectra of A particles (e) and B particles (f).

density at 1400 °C (Fig. 6) showed a lower hardness compared to Y-TZPA at 1400 °C and Y-TZP at 1500 °C. Taking into account that Y-TZP is harder than $ZrSiO_4$ ($H_v \sim 10–11$ GPa) and calcium phosphates ($H_v \sim 4–5$ GPa), these difference in the H_v values could be attributed to the greater amount of $ZrSiO_4$ and calcium phosphate secondary phases in sintered Y-TZPB.

The results show that the 64S decomposition during the sintering process of Y-TZPA and Y-TZPB compacts produced amorphous SiO_2 phase at the intermediate sintering stage which enhanced the densification. At 1300–1500 °C, $ZrSiO_4$ and calcium phosphate particles homogeneously distributed within the Y-TZP matrix were observed. Calcium phosphate bioceramics possess remarkable biocompatibility and bioactivity [17]; furthermore, their surfaces provide good conditions for osteoblast cells to adhere and proliferate [18]. Therefore, the in-situ formation of calcium phosphate in sintered Y-TZPA will have the potential to improve the Y-TZP biological properties without significantly altering its hardness; future in vitro studies will be conducted to study the effect of calcium phosphate particles in the biocompatibility of Y-TZP ceramics.

On the other hand, $ZrSiO_4$ exhibits excellent thermal shock resistance as a result of its very low thermal expansion coefficient and low heat conductivity coefficient [19]. In this sense, another aspect to

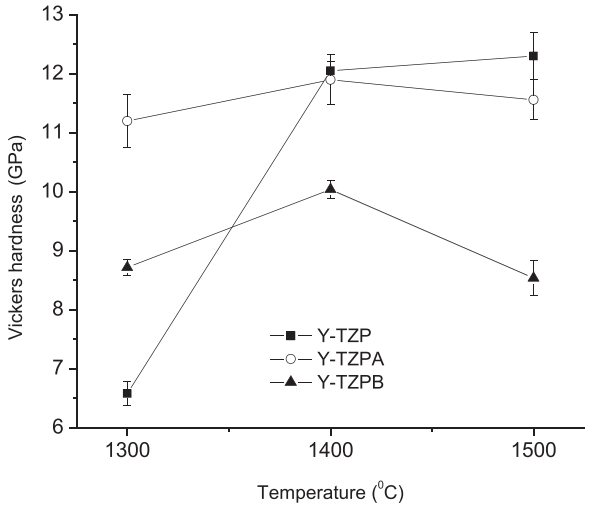

Fig. 10. Vickers hardness versus sintering temperature for Y-TZP, Y-TZPA and Y-TZPB compacts (10 °C/min heating/cooling rates).

investigate will be the thermal shock properties of the as designated sintered Y-TZP-64S for their potential use as structural ceramics.

4. Conclusions

The development of Y-TZP ceramics with 10.5 and 19.9 vol% 64S glass additions has been presented. $Ca_3(PO_4)_2$ along with SiO_2 as a major phase were obtained from thermal decomposition of the sol-gel derived 64S glass at 950–1500 °C. The SiO_2 phase markedly increased the Y-TZP solid state sintering rate at the intermediate stage; both 64S additions promoted the sintering process at a lower temperature with respect to Y-TZP (1500 °C). The rapidly cooling at 10 °C/min inhibited the t-m transformation of Y-TZP and markedly reduced that of Y-TZP-64S at 1300–1500 °C. Sintered Y-TZP with 10.5 vol% 64S, nearly fully densified at 1300–1400 °C, was constituted by polygonal $ZrSiO_4$ particles and elongated $Ca_2P_2O_7$ particles uniformly distributed in the tetragonal zirconia fine grain matrix. This ceramic exhibited similar hardness to that of Y-TZP sintered at 1500 °C; the in situ formation of calcium phosphate will have the potential to improve the Y-TZP biological properties without significantly affecting its hardness.

Acknowledgement

This work was financially supported by CONICET (PIP 0454).

References

[1] M. Guazzato, M. Albakry, S.P. Ringer, M.V. Swain, Strength, fracture toughness and microstructure of a selection of all-ceramic materials. Part II. zirconia-based dental ceramics, Dent. Mater. 20 (5) (2004) 449–456.
[2] A.F. Habibe, L.D. Maeda, R.C. Souza, M.J.R. Barboza, J.K.M.F. Dauano, S.O. Rogero, C. Santos, Effect of bioglass additions on the sintering of Y-TZP bioceramics, Mater. Sci. Eng. C 29 (2009) 1959–1964.
[3] C. Santos, R.C. Souza, A.F. Habibe, C.N. Elias, Mechanical properties of Y-TZP ceramics obtained by liquid phase sintering using bioglass as additive, Mater. Sci. Eng. A 478 (2008) 257–263.
[4] L.L. Hench, The story of Bioglass, J. Mater. Sci. Mater. Med. 17 (2006) 967–978.
[5] C. Piconi, G. Maccauro, Zirconia as a biomaterial, Biomaterials 20 (1999) 1–25.
[6] R.A. Young, "The Rietveld Method," International Un-ion Crystallography, Oxford University Press, Oxford, 1993.
[7] J. Rodríguez-Carvajal, Recent developments of the program FULLPROF, in Commission on powder diffraction (IUCr), Newsletter 26 (2001) 12–19.
[8] A. Le Bail, Modelling the silica glass structure by the Rietveld method, J. Non-Cryst. Solids 183 (1–2) (1995) 39–42.
[9] K. Sinkó, A. Meiszterics, J. Rohonczy, B. Kobzi, S. Kubuki, Effect of phosphorus precursors on the structure of bioactive calcium phosphate silicate systems, Mater. Sci. Eng. C 73 (2017) 767–777.
[10] A. Goel, S. Kapoor, R.R. Rajagopal, M.J. Pascual, H.W. Kim, J.M. Ferreira, Alkali-free bioactive glasses for bone tissue engineering: a preliminary investigation, Acta Biomater. 8 (2012) 361–372.
[11] K. Matsui, Sintering kinetics at constant rates of heating: mechanism of silica-enhanced sintering of fine zirconia powder, J. Am. Ceram. Soc. 91 (8) (2008) 2534–2539.
[12] Y. Sakka, Y. Oishi, K. Ando, Zr-Hf interdiffusion in polycrystalline Y_2O_3-$(Zr+Hf)O_2$, J. Mater. Sci. 17 (11) (1982) 3101–3105.
[13] N. Ohmichi, K. Kamioka, K. Ueda, K. Matsui, M. Ogai, Phase transformation of zirconia ceramics by annealing in hot water, J. Ceram. Soc. Jpn. 107 (2) (1999) 128–133.
[14] J. Zhao, Y. Ikuhara, T. Sakuma, Grain growth of silica-added zirconia annealed in the cubic/tetragonal two-phase region, J. Am. Ceram. Soc. 81 (8) (1998) 2087–2092.
[15] K. Matsui, H. Horikoshi, N. Ohmichi, M. Oghai, H. Yoshida, Y. Ikuara, Cubic-formation and grain growth mechanism in tetragonal zirconia polycrystal, J. Am. Ceram. Soc. 86 (8) (2003) 1401–1408.
[16] R.W. Rice, C.C. Wu, F. Borchelt, Hardness-grain size relations in ceramics, J. Am. Ceram. Soc. 77 (10) (1994) 2539–2553.
[17] S.V. Dorozhkin, Biphasic, triphasic and multiphasic calcium orthophosphates, Acta Biomater. 8 (2012) 963–977.
[18] M. H-Uoshima, I. Ishikawa, A. Kinoshita, H.T. Weng, S. Oda, Clinical and histologic observation of replacement of biphasic calcium phosphate by bone tissue in monkeys, Int. J. Peridontics Restor. Dent. 15 (1995) 205–213.
[19] C. Aksel, The influence of zircon on the mechanical properties and thermal shock behaviour of slip-cast alumina-mullite refractories, Mater. Lett. 57 (2002) 992–997.